

# FROM END-OF-LIFE TO IMPACT ON GROUND: AN OVERVIEW OF ESA'S TOOLS AND TECHNIQUES TO PREDICTED RE-ENTRIES FROM THE OPERATIONAL ORBIT DOWN TO THE EARTH'S SURFACE

*S. Lemmens<sup>1</sup>, B. Bastida Virgili<sup>2</sup>, V. Braun<sup>2</sup>, T. Flohrer<sup>1</sup>, Q. Funke<sup>2</sup>, H. Krag<sup>1</sup>, F. Mclean<sup>3</sup>, K. Merz<sup>1</sup>*

<sup>1</sup> Space Debris Office, ESOC, European Space Agency;

<sup>2</sup> IMS Space Consultancy GmbH at Space Debris Office, ESOC, European Space Agency;

<sup>3</sup> CS GmbH at Space Debris Office, ESOC, European Space Agency;

## ABSTRACT

Once an object in Earth orbit has reached the end of its operational life, or in case of a space debris object after its genesis, it enters into the re-entry prediction system of ESA's Space Debris Office. This system automatically predicts the remaining orbit lifetime. In case of a short remaining orbit lifetime it automatically predicts the impact location, risk and associated uncertainties; In case of a high risk re-entry event it enables the in-depth analysis of the affected regions and atmospheric break-up of the object. Tools are available for post-event processing of the observational data. The results of this analysis chain are provided to the relevant actors, e.g. national alert centres or operators, either automatically or on-demand.

In this paper we present the status of the re-entry prediction system, and its orbit determination, orbit propagation, environment forecasting, and risk assessment methodologies related to the orbital lifetime, re-entry location, and atmospheric break-up predictions. Uncertainties depending on the orbit regions, object type, and step in the re-entry prediction system are derived and used to tune the service to provide the best possible results over the entire population. In the last step of the system, these automatically generated results are complemented with an operator review of the available data to provide re-entry and break-up prediction for individual objects, occasionally complemented by processing dedicated observations of the re-entry object. Post-mortem analyses, e.g. after a confirmed re-entry, are performed for selected objects in order to explain potential observations of the re-entry event and retrieved samples on-ground. The entire data collection is a relevant source of information which serves as input for break-up modelling tools, and improvement of the entire prediction service.

*Index Terms*— Re-entry prediction

## 1. INTRODUCTION

Currently, there are about 17 000 tracked objects in Earth orbit, out of which approximately 7500 are estimated to have a remaining orbital lifetime of less than 100 years. Out of those 7500, about 1250 have a mass of more than 1 kg, but the vast majority are smaller pieces of space debris. For both categories, the importance of re-entry predictions has been established albeit targeting different issues. For small pieces of debris it is important to quantify and monitor their decent rate over the years as they pass through the orbits of operational satellites and as such increase the risk of collisions. For the less numerous but larger and heavier objects, of 500 kg and above, there is the risk that some parts of the spacecraft survive the re-entry and impact on ground. A rough estimate indicates that 10 to 40 % of large objects such as rocket bodies or satellites can survive until ground impact and thus are of special interest for civil protection agencies [8]. To perform re-entry predictions for all trackable objects in space the Space Debris Office of the European Space Agency (ESA) has set-up a Re-entry Prediction Service (RPS) which generates the data on a daily basis, together with a set of tools of environment modelling, optimisation, and a system for disseminating the results. The focus of this paper will be on the accuracy of the service as a whole, rather than fine-tuning for an individual object.

The subject of re-entry predictions is intimately linked with subject of orbital lifetime assessment prior to the launch of an object. This subject and associated tool are covered in depth in [2][3]. Both orbital lifetime assessments and re-entry predictions are heavily dependent on the ability to predict the further space weather environment as in the vast majority of the cases the re-entry is triggered by loss of orbital altitude due to interaction with Earth's atmosphere via the density parameter, which in turn is largely determined via space weather effects. However, a non-negligible amount of re-entries are triggered by the gravity of the Sun and Moon perturbing the object's orbit as well.

## 2. SPACE ENVIRONMENT MODELLING

In order to model the future solar radio frequency flux and geomagnetic evolution, which serve as input models to atmosphere models, ESA has developed its own solar and geomagnetic activity prediction model (SOLMAG), which uses data from past solar cycles to predict the future ones [12]. SOLMAG has a short term prediction algorithm covering the following solar month, with daily values for the predictions based on a neural network estimator, and a medium and long term prediction for the next centuries, with predicted values provided on a monthly basis. The medium and long-term prediction method implemented in SOLMAG is based on the technique of McNish and Lincoln, which is similar to that used by Holland and Vaughan. The default ESA prediction is generated using all data available from solar cycle 12 onwards, which is the cycle from which there were already both sunspot and geomagnetic activity observations. These predictions are taken as a given for the RPS. If required, this forecast can be replaced by the International Standard Organisation and European Cooperation for Space Standardization methodologies as described in [2].

The atmospheric model of choice for the current version of the RPS is the empirical US Naval Research Laboratory Mass Spectrometer and Incoherent Scatter Radar model NRLMSISE-00.

## 3. RE-ENTRY PREDICTIONS

The RPS consist out of ESA's Database and Information System Characterizing Objects in Space (DISCOS), which stores the results of the RPS and provides an interface to the object and orbital information, a tool for estimating the ballistic coefficient from orbital information, and propagators to estimate the re-entry date [5]. The first version of this tool chain became operational in October 1999 and has been under continuous development ever since [4]. The main input to the RPS is the public Two-Line Elements (TLE) catalogue maintained by United States Strategic Command (USSTRATCOM), in combination with information from other catalogues or dedicated observations when required. All approximately 17000 objects in the system are processed daily, taking into account the orbital information available from the previous days. During the last 60 days, the entire TLE catalogue is used. Older input elements are sampled down to a state every week. The whole service, which will be described below in detail, runs on a single-core Linux server in under 10 hours. Access to the predictions is available for registered users via e-mail, with a public web portal under development.

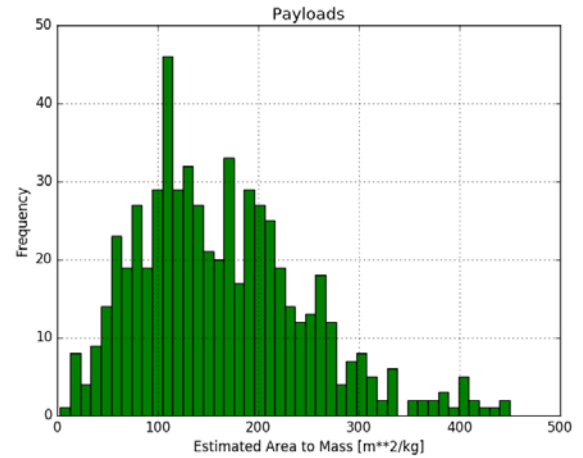


Figure 1: Estimated  $B/c_D$  for payloads.

### 3.1. Ballistic Parameter Estimation

In order to make a re-entry prediction, the RPS estimates the ballistic parameter ( $B$ ) of the object by analysing the orbital position history. Concretely, an iterative shooting method is applied to the orbital states within a time span  $\Delta T$  whereby one searches the value

$$B = c_D \frac{A}{m},$$

where  $A$  is the cross-sectional area,  $m$  the mass, and  $c_D$  the drag coefficient of the object, such that the positional error while propagating from one observed orbital state to a consecutive one is minimised. For this procedure the object is assumed to be in the free molecular flow regime and  $c_D$  is fixed to 2.2. The time span parameter  $\Delta T$  is accompanied with a second time span parameter,  $\delta T$ , which defines the minimum time between two orbital states used for the shooting method. The maximum amount of pairs generate this way is limited and  $B$  is first computed from the pairs which are closest in time. After computing  $B$  for all possible pairs within  $\Delta T$ , the estimated  $B$  used for further propagating is the mean value of the  $B$ s for all pairs. The standard deviation is computed as well and can serve to detect manoeuvring objects. As input to this method the ballistic parameter derived from the geometric data available in DISCOS is used. This methodology only applies to objects which spend time in orbits with enough residual atmosphere, which is arbitrary limited to a perigee altitude below 1000km. Above, the geometric cross-section stored in DISCOS is used as estimate for the re-entry prediction.

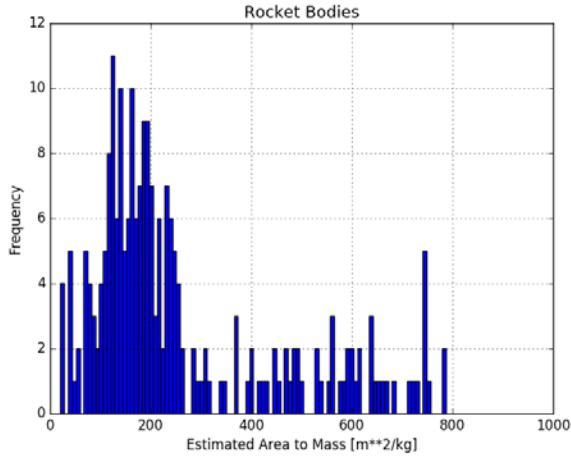


**Figure 2: Estimated  $B/c_D$  for rocket bodies.**

In Figure 1 and Figure 2 the results for the estimation process are shown for all rocket bodies and payloads which meet the criteria and have standard deviation of less than 50% of the mean value. In Figure 3 the ratio between the estimated  $B$  and the geometric  $B$  is given for the same objects. The large majority is contained between 0 and 2, and hence in good agreement. The outliers can be explained by pointing out that the shapes in DISCOS, and hence the derived areas, are for a significant amount of cases based on the average of known similar spacecraft [5]. However, they are within limits for the shooting method to converge.

The accuracy of the shooting method however depends critically on the selection of the parameters  $\Delta T$  and  $\delta T$ , which can be significantly different for distinct orbital regimes. To analyse these effect, one can use the knowledge of past re-entries to compare which estimate  $B$  brings the re-entry prediction closest to the actual re-entry. E.g. in order to characterise the orbits for which re-entries are expected within weeks to months, 27 Flock satellites of the Planet Labs cubesats constellation released from the International Space Station were identified as candidates due to having the identical design, varying orbital node, only using limited differential drag for constellation maintenance, and availability of frequently updated orbital states [6]. For all 27 object the parameters  $\Delta T$  and  $\delta T$  are varied between 5 and 110 days, and 1 and 36 days respectively, for initial estimation altitudes between 200 and 350 km. For each estimated  $B$  a semi-analytical propagator outside the RPS was used to predict the re-entry epoch, which was then used to derive the prediction error ( $E_P$ ):

$$E_P = \left| \frac{Epoch_{predicted\ re-entry} - Epoch_{actual\ re-entry}}{Epoch_{prediction} - Epoch_{actual\ re-entry}} \right| \cdot 100$$

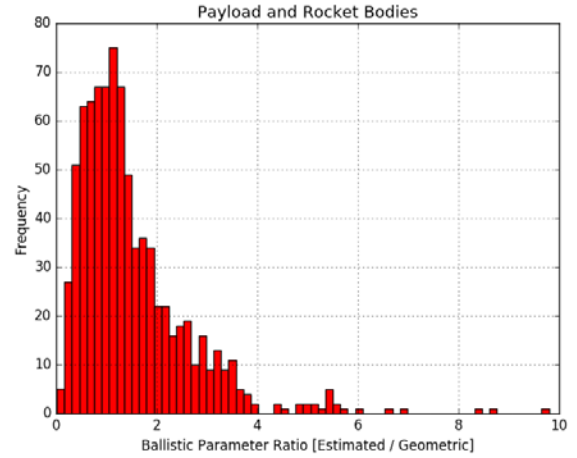


**Figure 3: Ratio of estimated to geometric  $B$  for payloads and rocket bodies.**

The results are then aggregated over all satellites for each variation of the parameters and orbital altitude by taking the median of the  $E_P$ s. This analysis implicitly absorbs the effects of the sensor network used to generate the data by selection of the objects in general. Also the prediction and re-entry epochs at the same altitudes for the individual objects can, and nearly always are, different.

In Figure 4 two examples are given of the procedure: One at the orbital altitude of 320 km and one at 200km. It clearly shows the existence of preferential regions for the selection of the parameters, which systematically outperform the other regions in all 10 km altitude steps. Similar analyses have been undertaken for objects on higher Low Earth Orbits (LEO) altitudes, without inclination restrictions, and for Ariane upper stages in Geostationary Transit Orbits (GTO). For the former some regions of good accuracy could be found per altitude slice but these regions would move between the slices, indicating that a larger dataset might be required. Only 24 objects were used for the high LEO case. In case of the 33 GTO objects a strong correlation could be noted between the existence of good accuracy regions and the orbital geometry, i.e. correlating with the sensors network generating the data, confirming the difficulties with re-entry predictions for GTO's in general.

In general it can be pointed out that the RPS can ingest ballistics parameters from other estimation processes, e.g. from direct orbit determination. This is required to improve the accuracy close to re-entry or for highly eccentric orbits, as in case of the former long  $\Delta T$  periods lose their benefits and for the later quality filtering only leaves few orbital state pairs as input for the estimation process.

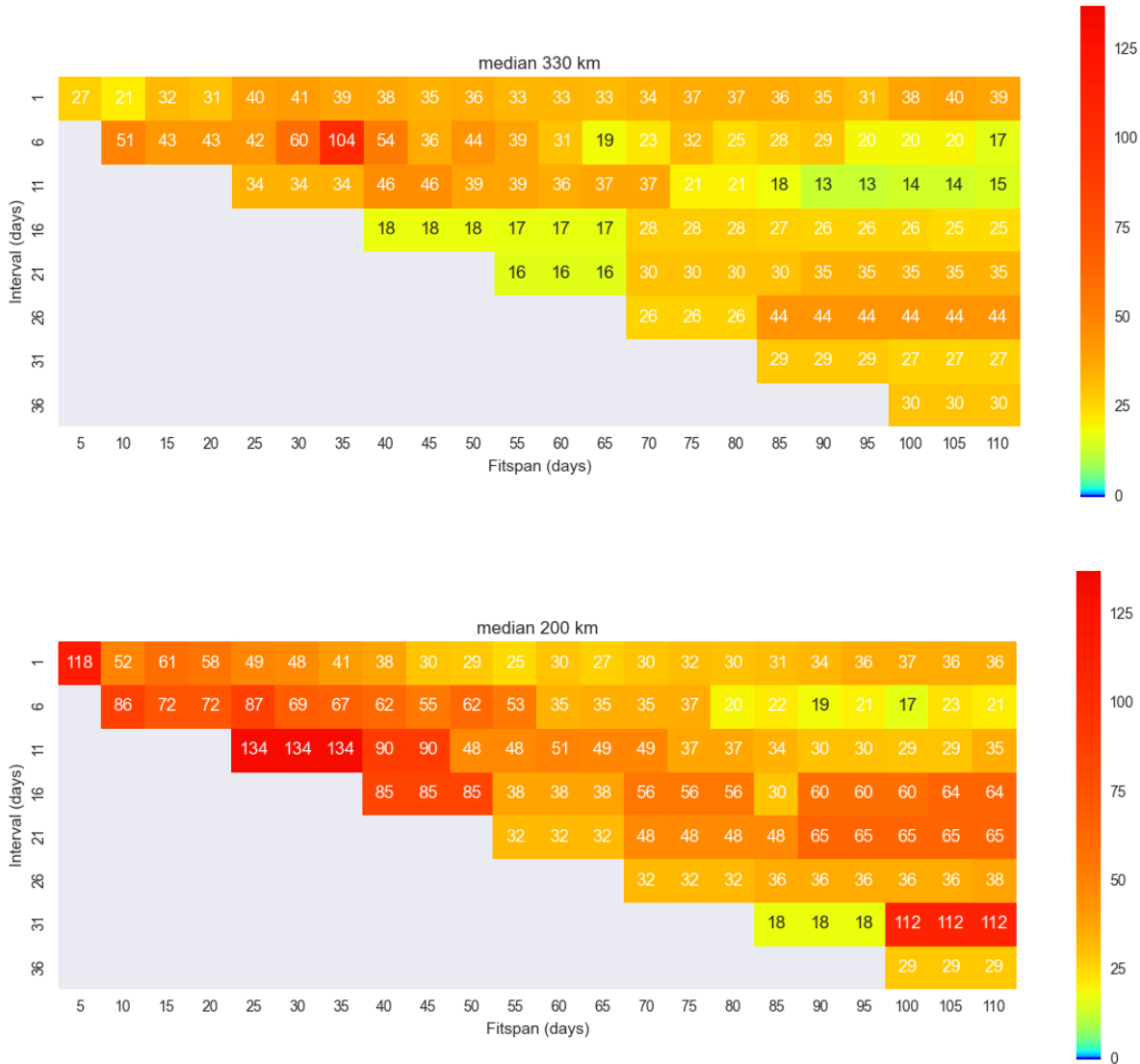


**Figure 4: Median  $E_p$  used to assess the accuracy of the estimated  $B$  for different orbital regime and parameters based on 27 Flock satellites.**

### 3.2. Long-term Re-entry Predictions

For any new object entering the RPS, an initial estimate of the re-entry epoch is made by an analytic propagator based on applying the King-Hele equations for lifetime calculations given the initial density at perigee [7]. In the case of long-term re-entry predictions, i.e. where the object has an orbital lifetime of more than two solar cycles, the use of a numerical or even semi-analytical propagator is no longer advisable vis-à-vis the associated uncertainties and the computational load. In case the derive re-entry epoch from the analytical propagator is further away than 1000

years, the process stops and the estimate is stored. In case of a shorter orbital lifetime, the analytical theory is applied iteratively by sampling the density at perigee during various steps within the solar cycle w.r.t. a the static CIRA72 atmosphere model. Objects which have a long orbital lifetime via these analytical methods and a high orbit eccentricity are recomputed with the semi-analytical method, which is described for short term re-entry predictions, to increase accuracy. Based on these methods Figure 5 represent the computed orbital lifetime for payloads and rocket bodies on circular LEO orbits. Satellites constellations in higher LEO orbits can be easily discerned.

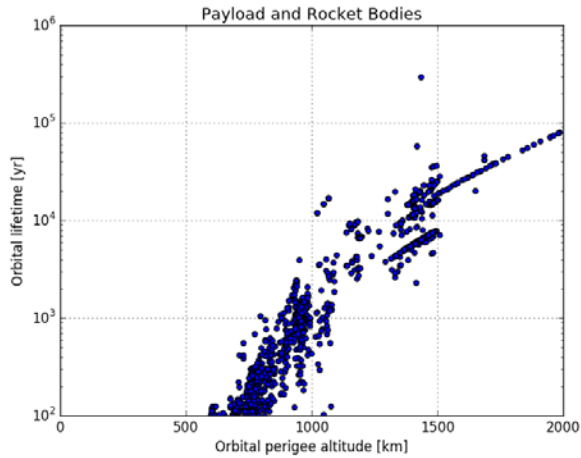


**Figure 5: Long term orbital lifetimes versus perigee height for non-maneuvering object on circular LEOs.**

### 3.2. Short-term Re-entry Predictions

To automatically monitor and forecast the orbit evolution of a re-entering object over periods of several years to a few weeks of remaining lifetime, i.e. less than a few solar cycles, computationally efficient yet sufficiently accurate methods must be applied. For this purpose ESA uses a semi-analytical propagator called Fast Orbit Computation Utility Software (FOCUS). The propagator integrates the combined time rates of change of singly averaged perturbation equations, taking into account a non-spherical Earth gravity potential, a dynamic Earth atmosphere, luni-solar gravity perturbations, and solar radiation pressure in combination with an oblate, cylindrical Earth shadow. The integration is performed by a robust fourth-order Adams-Bashforth-Moulton predictor/corrector method, which is initiated by a self-starting fourth-order Runge-Kutta-Fehlberg method, using fixed time steps of 0.1 to 5 orbits, depending on the time to go until re-entry [8].

For the automated short-term re-entry predictions by the RPS of intact objects, the goal is to have a daily update on the potentially affected areas and date of the re-entry. Accuracy down to the day combined with an uncertainty on the ground track of multiple revolutions is in general sufficient as starting point of a deeper analysis if required, and serves the need of the general public on the awareness of re-entry events. Due to the variability in the  $B$  estimation reported earlier, combined with the variability in the lower atmosphere which is averaged in most atmosphere models for altitudes below 400km, automated short-term re-entry prediction can be rather volatile in terms of  $E_p$  as shown in Figure 6.

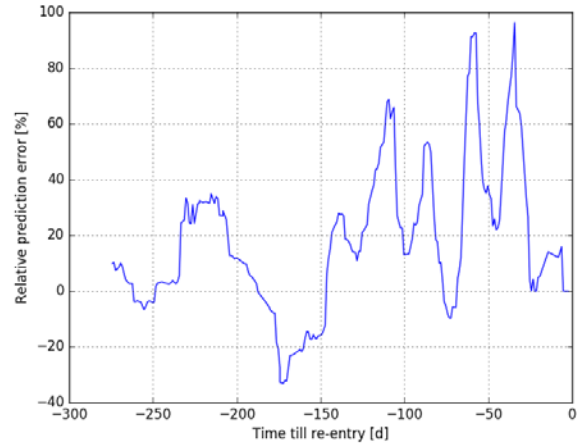


**Figure 6: Example of an automated short-term re-entry for a S3M rocket body prediction based on FOCUS in terms of  $E_p$ .**

The objectives of automated re-entry predictions are in sharp contrast to manual detailed re-entry predictions for individual objects where the goal is to accurately predict the re-entry location and date. This can include the scheduling of dedicated sensors and furthermore requires operator involvement to aid in the prediction process. In this case, the  $B$  is estimated by using FOCUS in estimation mode. Herein  $B$  is again estimated by a shooting method between orbital state pairs as before, and refined based on minimisation of the derived orbit w.r.t. to the semi-major axis and argument of latitude of the observation elements. Furthermore for the final leg of the re-entry prediction, i.e. when moving from the rarefied to the continuum flow regime, the propagator FOCUS is replaced by a full numerical integrator, OrbGen, which also takes into account the variation in  $c_D$  due to the changes in flow regime and propagates the state until ground impact. This manual procedure leads to the figure of 20% uncertainty on the remain orbital lifetime at the prediction epoch, which is considered the state-of-the art for re-entry predictions [8]. However, in practice the accuracy of manual re-entry predictions can be even as low as 5% under certain conditions [10].

The question then becomes if the manual procedure can be automated or at least how far, as this would increase the RPS accuracy for certain classes of objects of special interest. To this end, the procedure above is run with a fixed amount of orbital states, 20, for all payloads or rocket bodies with a mass above one ton. The improvements in the re-entry prediction can be significant, as is visible in Figure 7, were the same object as in Figure 6 was analysed and the  $E_p$  halved during the overlap period near the final re-entry.

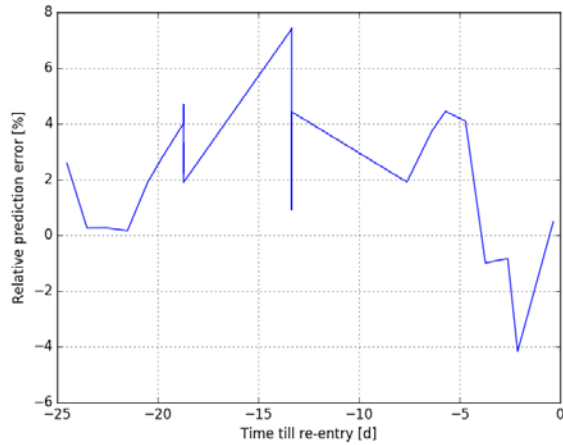


**Figure 7: Example of an automated short-term re-entry for a S3M rocket body prediction based on FOCUS/OrbGen in terms of  $E_p$ .**

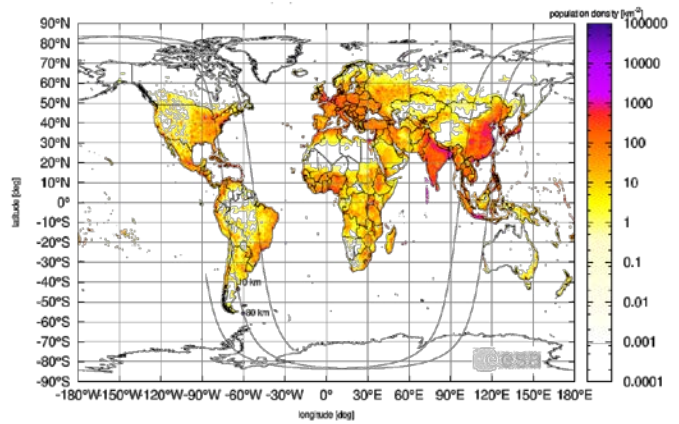


**Figure 9: Re-entry prediction ground track interpreted as uncertainty.**

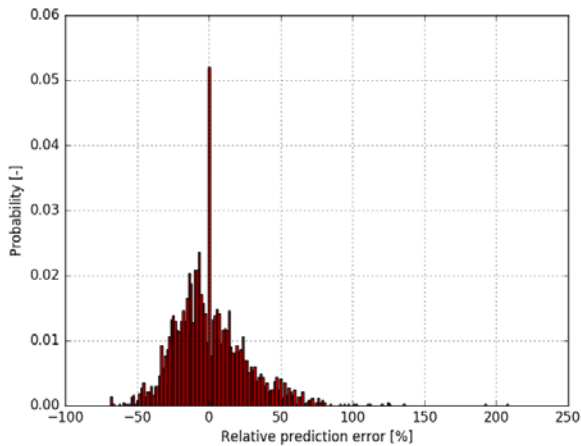


**Figure 8: Distribution of  $E_p$  for the automated FOCUS re-entry predictions.**

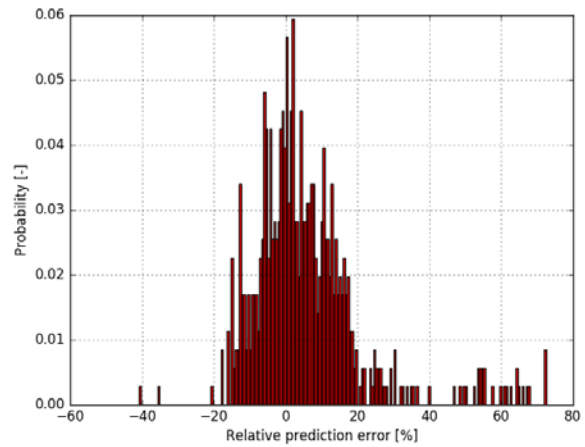


**Figure 10: Distribution of  $E_p$  for the augmented FOCUS/OrbGen re-entry predictions.**

To systematically check if the change in procedure leads to results on the par with manual predictions, a comparison can be made between the two procedures where we compute the  $E_p$  for all payloads or rocket bodies involved and compare predictions to the re-entry epoch as reported by Joint Space Operations Center (JSpOC) via the interface [www.space-track.org](http://www.space-track.org). This is done only where JSpOC reported the uncertainty on the re-entry epoch to be less than 10min, i.e. it is assumed the re-entry was observed. For the standard automated re-entry predictions based on FOCUS, objects with an eccentricity above 0.1 were excluded and only the last 50 days prior to the re-entry were used. This retained 62 objects with a re-entry epoch between 2014 and 2016. For augmented re-entry predictions based on FOCUS & OrbGen

no objects were excluded and time spans up to 80 days prior to the re-entry were used. This retained 25 objects with a re-entry epoch between 2014 and 2016. The results of the comparison based on  $E_p$  are presented in Figure 8 and Figure 10. In case of the automated predictions based on FOCUS, we observe a right-sided heavy-tail distribution between -50% and 70% centred on 0%, whereas for the augmented predictions we observe a right-sided heavy-tail distribution between -20% and 30% centred on 0%. The latter clearly outperforms the former, even with the inclusion of eccentric objects which cause the positive outliers. Identifying the shape of the distribution has its potential application to the calculation of the ground track affect by a re-entry as in Figure 9.

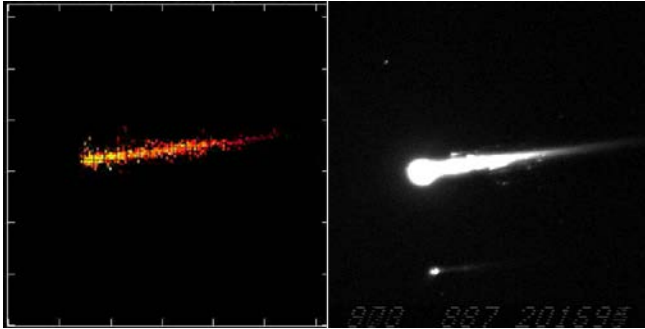


**Figure 11: RENFOT simulation and observation for the ATV-1 re-entry campaign.**

#### 4. POST RE-ENTRY ANALYSES

For larger and heavier spacecraft, such as payloads and rocket bodies, the re-entry prediction is not the end of the story but the chance exists that their interaction with the atmosphere is observed from ground or parts of the spacecraft are found and retrieved. Since the beginning of the space age a few hundred of re-entry events have been reported and less than a hundred re-entry events have occurred where debris pieces were at least tentatively identified as belonging to a spacecraft. Of those debris pieces the vast majority were pressure vessels.

Re-entry sightings become more frequent and even dedicated observations campaigns are being organised for objects of interest. The Re-ENtry FoOTprint (RENFOT) tool was developed to help the validation process for ESA's model for re-entry survivability and on-ground risk assessment for explosive re-entry events using the observation data [1]. The underlying rationale is to improve the models for the benefit of planning and execution of future controlled re-entries and risk calculations in case of uncontrolled ones. Validation obtained by comparing synthetic images generated by integrating the heat of fragments, as predicted by break-up software, and computing how this would be observed, by an airborne or land based camera, to real observations. The level of agreement between the forward modelling approach and the actual observation is derived qualitatively. The ATV-1 re-entry campaign served as a test bed for the combination of ESA's Spacecraft Entry Survival Analysis Module (SESAM) code in combination with NASA's EVOLVE 4.0 explosion model, whereas a still image of the break-up of ESA's GOCE satellite was compared with a simulation from ESA's SpaceCraft Atmospheric Re-entry and Aero-thermal Break up (SCARAB) software [9][11]. Examples for both comparisons are given in Figure 11 and Figure 12.

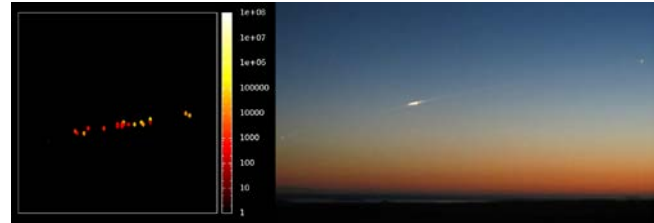


**Figure 12: RENFOT simulation and observation for the GOCE re-entry campaign.**

For a given re-entry prediction where ground impacting pieces are expected, the use of an object-oriented spacecraft break-up tool such as SESAM can be instructive for the identification of fragments and the affected area in case a search would be required. As an example of this potential, we point to the presumed re-entry of a rocket body over Spanish territory on the morning of 2015-11-03 around 6 UTC. Five pieces of space debris have been found on-ground between 2015-11-03 and 2015-11-16 which could be tentatively linked to this re-entry event and enabled the identification of candidates for the re-entering spacecraft. When defining candidates for the unknown rocket body, a re-entry break-up simulation can be run which tries to mimic the ground track of the event and match the impact locations of the known fragments. The situation is shown in Figure 13. Via this optimisation, three more pieces would be expected, including a pressure tank which would accompany the tanks identified on ground. This pressure tank was reported to be found on 2016-03-08, fully matching the expected ground track and positioned as predicted w.r.t. to the earlier found debris pieces.

#### 5. SUMMARY AND OUTLOOK

The first version of ESA's Space Debris Office RPS was setup in 1999 and has undergone some drastic changes and maintenance since then. The most important of those changes is that the entire public catalogue of orbital states of USSTRACOM, currently containing approximately 17000 objects, is processed daily to predict the re-entry date of the objects contained within. Automatically processing this large amount of data requires the careful derivation of global settings, e.g. for the derivation of the ballistic parameter for each object from its orbital decay rate when possible. Equally important is the selection of orbit propagators suited to the desired accuracy.

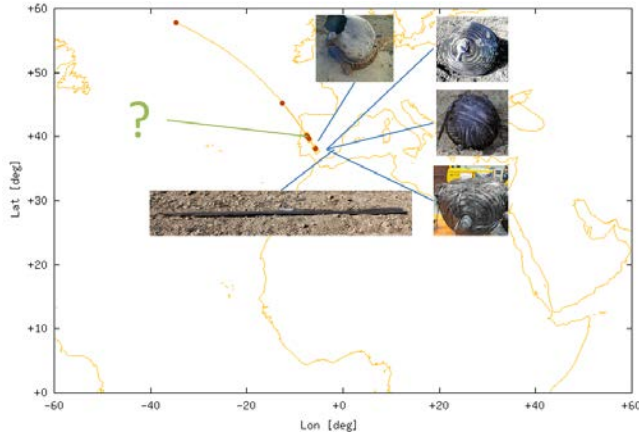


**Figure 13: Objects related to the re-entry of a rocket body over Spanish territory during November 2015.**

We have shown that for large objects near re-entry the automated process can be setup in such a way that it is on the par with a manual re-entry prediction, specifically by reaching the 20% relative error accuracy. This level of accuracy is a requirement for deriving optimal gain for post re-entry analysis which can be used for software validation as well as identifying pieces on ground.

However further developments to the RPS remain imperative. For one the pre-filtering of orbital states prior to the re-entry prediction methodology has shown advantages over statistically absorbing the errors in the parameter. Also for objects with a low  $B$  parameter studies have indicated that a significant loss in prediction accuracy near re-entry can be offset by using 6 degrees of freedom (DoF) propagators instead of the nominal 3 DoF propagators. An examples is given in Figure 14.

## 6. REFERENCES

[1] B. Bastida Virgili, H. Krag, T. Lips, and E. De Pasquale, "Simulation of the ATV Re-Entry Observations", *Proceedings of the 4<sup>th</sup> IAASS Conference*, ESA, Huntsville, United States, May 2010.

[2] V. Braun, et al, "Upgrade of the ESA DRAMA OSCAR Tool: Analysis of Disposal Strategies Considering Current Standards for Future Solar and Geomagnetic Activity", *Proceedings of the 6<sup>th</sup> European Conference on Space Debris*, ESA, Darmstadt, Germany, April 2013.

[3] V. Braun, et al, "Probabilistic Orbit Lifetime Assessment with OSCAR", *Proceedings of the 6<sup>th</sup> International Conference on Astrodynamics Tools and Techniques*, ESA, Darmstadt, Germany, March 2016.

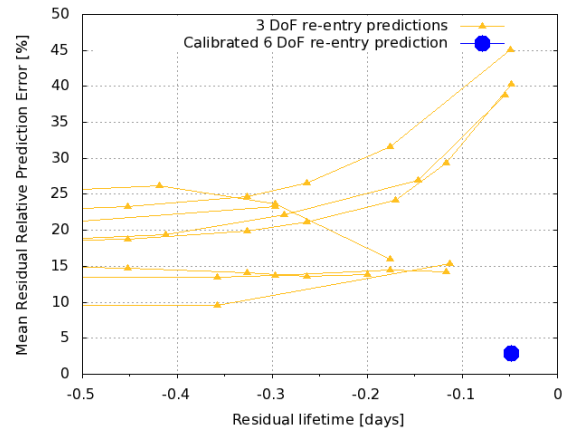


**Figure 14: Comparison of 3 and 6 DoF re-entry predictions for objects with a low  $B$ .**

[4] K. D. Bunte, H. Sdunnus, J.C. Mandeville, and H. Klinkrad, "Ballistic Parameter and Lifetime Assessment for Catalogued Objects", *Proceedings of the 3<sup>th</sup> European Conference on Space Debris*, ESA, Darmstadt, Germany, March 2001.

[5] T. Flohrer, et al, "DISCOS: Current Status and Further Developments", *Proceedings of the 6<sup>th</sup> European Conference on Space Debris*, ESA, Darmstadt, Germany, April 2013.

[6] C. Foster, H. Hallam, and J. Mason, "Orbit Determination and Differential-drag Control of Planet Labs Cubesat Constellations", *Proceedings of the AIAA Astrodynamics Specialist Conference*, AIAA, Vale, United States, August 2015.

[7] D.G. King-Hele, *Satellite Orbits in an Atmosphere: Theory and Application*, Blakie and Son Ltd, United Kingdom, 1987.

[8] H. Klinkrad, *Space Debris: Models and Risk Analysis*, Springer-Verlag, United Kingdom, 2006.

[9] G. Koppenwallner, B. Fritsche, T. Lips, and H. Klinkrad, "Scarab - a Multi-Disciplinary Code for Destruction Analysis of Space-Craft during Re-Entry", *Proceedings of the 4<sup>th</sup> European Conference on Space Debris*, ESA, Darmstadt, Germany, April 2005.

[10] S. Lemmens, et al, "Calibration of radar based re-entry predictions". *Proceedings of the 5th International GOCE User Workshop*, ESA, Paris, France, November 2014.

[11] C. Martin, et al, "a Debris Risk Assessment Tool Supporting Mitigation Guidelines", *Proceedings of the 4<sup>th</sup> European Conference on Space Debris*, ESA, Darmstadt, Germany, April 2005.

[12] R. Mugellesi-Dow, et al, "SOLMAG: an operational system for prediction of solar and geomagnetic indices", *Proceedings of the 1<sup>st</sup> European Conference on Space Debris*, ESA, Darmstadt, Germany, April 1993.